ROBUST DAMAGE PREDICTION OF LAMINATED OPEN-HOLE STRUCTURES

J. Germain[1], J. Rannou[1], F. Laurin[1] and D. Martini[2]

[1]ONERA / DMAS ,Université Paris Saclay , F-92322 Châtillon – France
Email: jeremy.germain@onera.fr, johann.rannou@onera.fr, frederic.laurin@onera.fr
[2]Dassault Aviation, 78 Quai Marcel Dassault, 92210 Saint-Cloud – France
Email: dominique.martini@dassault-aviation.com

Keywords: damage, open-hole, modelling, finite-element method, failure.

Abstract

Damage and failure modelling of laminated composite structures has already been extensively studied. A lot of advanced models are available in the litterature, some of them are able to describe complex failure scenarios. However, their identification procedures are complex and they suffer from insufficient numerical robustness, avoiding their transfer to the industry.
In this paper, a new model which relies on a previous approach developed by ONERA in the World Wide Failure Exercice (WWFE-III) is proposed. The model remains physically based in the sense that damage variables represent physical quantities that can be experimentally measured. Application to T700GC/M21 illustrates that the identification procedure has been significantly simplified and can be performed in an industrial context. The mathematical complexity of the model has also been reduced in order to focus on first order degradation phenomena prior to failure. Finite elements computations show however that a special care needs to be taken to avoid spurious oscillations in the damage and stress fields.

1. Introduction

Industrial strength predictions of open-hole structures often exhibit a narrow range of validity. Since they are based on linear elastic modelling, they are not able to capture essential damage features which play a major role on these predictions. It is thus necessary, for each materials, to calibrate the modelling parameters on a large and costly experimental database with different, lay-ups, hole diameters (φ) or width/diameter ratios (w/φ). This ratio has not been studied in the litterature and may have an important effect on open-hole strength.
For this reason, Dassault Aviation and ONERA have started the collaborative research project MARCOS since September 2016, which aims at improving predictive capabilities and robustness of composite material modelling to simulate composite structures up to failure and especially open-hole plates. A lot of advanced models have already been proposed in the scientific community. They mainly rely on experimental observations and account for physically based degradation mechanisms [1-2]. Nevertheless, they suffer from complex identification procedures and insufficient numerical robustness from an industrial point of view.
The objective of this paper is to present a robust model for the prediction of damages that occur in open-hole specimens prior to failure. It relies on a previous approach developed by ONERA in the World Wide Failure Exercice (WWFE-III). The model remains physically based in the sense that damage variables represent physical quantities that can be experimentally measured. Simplifications are achieved by focusing on first order phenomena prior to failure.
In this paper, this continuum damage model is described. It is defined at the ply scale and relies on variables that can be observed during experimental tests. Its formulation is presented in section 2 and section 3.1 presents its identification procedure performed on T700GC/M21 thanks to previous

experimental campaign led at ONERA. The model predictive capabilities on stress gradient-free specimens are then evaluated in section 3.2. Section 3.3 is dedicated to finite element modelling of an open-hole tensile test and the associated numerical difficulties are discussed.

2. An advanced damage model for laminated composite materials

A physically based continuum damage model is proposed. It is defined at the ply scale. The complexity of the model and of its identification procedure have been intentionally restricted in order to improve its robustness. Emphasis has been put on describing damage mechanism known as matrix cracking. Fiber direction remains elastic. Complementary non-linear mechanisms such as fiber failure or delamination may be introduced later depending on open hole tensile simulation results with respect to experimental ones, on a wide range of specimens. Material behaviour is given by Eq. 1 where $\underline{\sigma}$ represents the stress, $\underline{\underline{\tilde{C}}}$ denotes the effective stiffness tensor while $\underline{\underline{\tilde{S}}}$ denotes the effective compliance tensor (discussed in section 2.1), $\underline{\varepsilon_{ve}}$ the viscous strain (discussed in section 2.2) and $\underline{\varepsilon_{th}}$ the residual thermal strain.

$$\underset{\sim}{\sigma} = \underset{\approx}{\tilde{C}} : (\underset{\sim}{\varepsilon} - \underset{\sim}{\varepsilon}_{ve} - \underset{\sim}{\varepsilon}_{th}) \Leftrightarrow (\underset{\sim}{\varepsilon} - \underset{\sim}{\varepsilon}_{ve} - \underset{\sim}{\varepsilon}_{th}) = \underset{\approx}{\tilde{S}} : \underset{\sim}{\sigma} \tag{1}$$

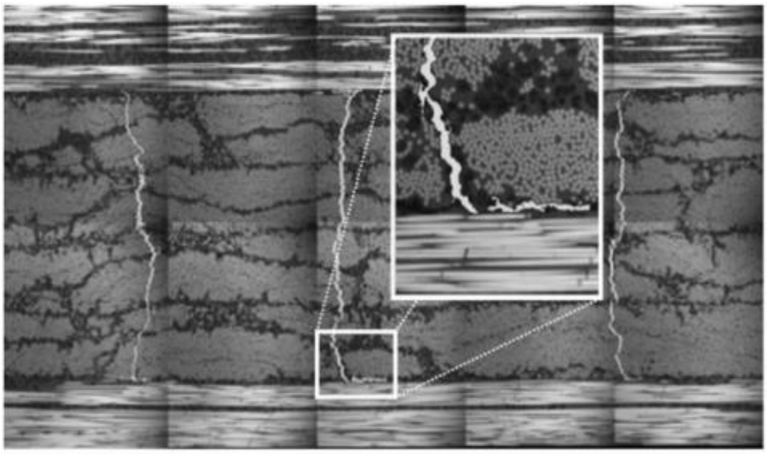

Figure 1. Transverse cracks and its associated micro-delamination observed on T700GC/M21 [3]

One key feature of the WWFE-III and the present model is that the damage is represented by a ply crack density that can be optically observed during tests on the edges of the specimen as shown in Fig. 1. These matrix cracks are due to the development and coalescence of micro-damages such as fibre/matrix debonding as experimentally observed by [3] and simulated by [4]. These direct observations allow for an accurate identification of damage thresholds and kinetics.The damage variables are ρ, which is the crack density and μ, the length of local delamination at the crack tip. In the following, the normalized $\bar{\rho}$ and $\bar{\mu}$ are considered in the model, as proposed in [5] and defined by Eq. 2, where h stands for the ply thickness and L the length between two consecutive cracks.

$$\begin{cases} \bar{\rho} & = \rho h \\ \bar{\mu} & = \frac{\mu}{L} \end{cases} \tag{2}$$

2.1. Mesoscopic damage formulation

The damage driving force is defined by Eq. 3 where $\underline{\sigma^+}$ is the positive part of a specific stress tensor composed by the stress components that may induce transverse cracking, all other stress components are set to zero. The distinction between transverse and shear stress contributions in damage driving force is taken into account through coefficients a_{24} and a_{26}.

$$Y = \frac{1}{2}\left(\sigma_{22}^{+\,2} S_{22}^0 + a_{24}\tau_{23}^{+\,2} S_{44}^0 + a_{26}\tau_{12}^{+\,2} S_{66}^0\right) \tag{3}$$

Damage evolution law is defined in Eq. 4. Damage onset Y_0 is a function of the ply thickness as the transverse and shear strengths are subjected to the so-called *in-situ* effect [6-7]. These strengths are computed according to [8]. Contrary to the previous approach, damage onset is not a function of the micro-damage variable (discussed in section 2.2). Consequently, this new model is easier to implement in a finite-element code.

$$\begin{cases} \bar{\rho} &= (1-\bar{\mu})h\alpha\langle Y - Y_0\rangle_+^p \\ \bar{\mu} &= \langle a_h\bar{\rho}^2 + b_h h\bar{\rho}\rangle_+ \end{cases} \tag{4}$$

Coefficients α and p are parameters controlling damage kinetic and $\langle\ \ \rangle_+$ are Macaulay brackets. It has been experimentally observed (as in [3]) that damage evolution remains influenced by the ply thickness h, hence its presence in Eq. 4. The coupling between $\bar{\rho}$ and $\bar{\mu}$ has been observed experimentally [3], it is used for the transverse crack density saturation. a_h and b_h are material coefficients which have to be identified.
Then, damage effect on the elastic compliance tensor is expressed by Eq. 5, $\underline{\underline{H_a}}$, $\underline{\underline{H_b}}$ and $\underline{\underline{H_c}}$ are three effect tensors which are built by solving multiple finite element periodic elastic problems on an elementary cracked cell [3].

$$\underset{\approx}{\tilde{S}} = \underset{\approx}{S}_0 + \underset{\approx}{H}_{meso} = \underset{\approx}{S}_0 + \bar{\rho}\underset{\approx}{H}_A + \frac{\bar{\mu}}{1-\bar{\mu}}\underset{\approx}{H}_B + \frac{\bar{\rho}^2}{1-\bar{\mu}}\underset{\approx}{H}_C \tag{5}$$

2.2. Viscoelasticity with micro-damage

The second source of non-linearity used in this model is the viscoelasticity. Indeed prior to the first transverse crack, an important material non-linearity is observed especially for shear loadings, and is assumed to be due to the viscosity of the matrix and micro-cracks.Using a non-linear viscoelastic behaviour allows to describe this non-linearity and takes into account the loading rate dependency of the behaviour. The behaviour is set non-linear by taking into account the effects of a micro-damage variable δ_2 and of matrix cracking (Eq. 6). In $\underline{\underline{\widetilde{S_r}}}$, the micro-damage variable effect, $\underline{\underline{H_{micro}^{ve}}}(\delta_2)$, increases the initial viscous compliance $\underline{\underline{S_{r0}}}$, prior to the mesoscopic transverse cracking effect $\underline{\underline{H_{meso}^{ve}}}(\overline{\rho},\overline{\mu})$, leading to a non-linear behaviour before the first transverse crack onset. The micro-damage variable δ_2 describes fibre/matrix debonding occurring in early stages of loading that is assumed to be responsible for the non-linear shear behaviour before the first transverse crack onset. Its evolution law is given in Eq. 7. Y_m is defined in a similar manner as for the mesoscopic damage driving force (see Eq. 3), where a_{24m} and a_{26m} are coefficients of the driving force, computed thanks to the shear stress inducing the non-linear behaviour. Y_{0m} is the micro-damage threshold and is necessary lower than the mesoscopic damage threshold Y_0. p_m and Y_{cm} are coefficients controlling micro-damage evolution.

$$\underset{\approx}{\tilde{S}}_r = \underset{\approx}{S}_{r0} + \underset{\approx}{H}^{ve}_{micro}(\delta_2) + \underset{\approx}{H}^{ve}_{meso}(\bar{\rho}, \bar{\mu}) \tag{6}$$

$$\delta_2 = \delta_{2max}\left(1 - \exp^{\left(\left(\frac{\langle Y_m - Y_{0m}\rangle_+}{Y_{cm}}\right)^{pm}\right)}\right) \tag{7}$$

The viscoelastic behavior is described by a spectral approach [9]: the ply viscosity is related to the contribution of N elementary viscous mechanisms as reported in Eq. 9. The ith viscous mechanism is defined by a relaxation time τ_i and a specific weight μ_i associated to a gaussian function whose parameters are n_0 and n_c. $\underline{\underline{\tilde{S_r}}}$ is a fourth order tensor representing the effective viscous compliance of the material, defined in Eq. 7.

$$\begin{cases} \dot{\underset{\sim}{\varepsilon}}_{ve} = \sum_{i=1}^{N} \dot{\underset{\sim}{\xi}}_i \\ \dot{\underset{\sim}{\xi}}_i = \frac{1}{\tau_i}(\mu_i \underset{\approx}{\tilde{S}}_r : \underset{\sim}{\sigma} - \underset{\sim}{\xi}_i) \\ \text{with } \tau_i = exp(i) \text{ and } \mu_i = \frac{1}{n_0\sqrt{\pi}} exp(-(\frac{n_i - n_0}{n_c})^2) \end{cases} \tag{8}$$

3. Numerical simulations

3.1. Damage model implementation and identification procedure

This model was implemented in an implicit finite element code, Z-Set/Zebulon, codeveloped by ONERA and Mines PARISTECH. As this model is stress-based, a local Newton-Raphson algorithm is needed to achieve internal variable convergence ($\bar{\rho}$ and $\underset{\sim}{\sigma}$). The Jacobian associated to the local Newton-Raphson algorithm and the consistent tangent stiffness matrix were analytically computed and checked through comparisons with the solution obtained using a numerical differentiation. It is important to note that the provided tangent stiffness matrix is non-symmetrical.

This model was identified on T700/M21 (268 g/m²) thanks to tests previously performed at ONERA [3].In order to completely identify the in-plane damage part of this model, a limited number of tests is required: at least two [0/90*n*/0] laminates with different amount of 90° plies clustered together and a $[+45/-45]_{2s}$ laminate.

Transverse in-situ strengths are identified on [0/90n/0] laminates and used to determine damage onset threshold Y_0 with Eq. 3 considering a pure transverse stress for different ply thicknesses.

The damage evolution law parameter α, p, a_h and b_h are identified from measurements of the crack density and the micro-delamination length at the crack tip with optical system on the edge of the [0/90*n*/0] specimens. As observed in Fig. 2 the proposed approach is able to accurately predict the onset and evolution of transverse cracking and of the associated micro-delamination length, as a function of the ply thickness.

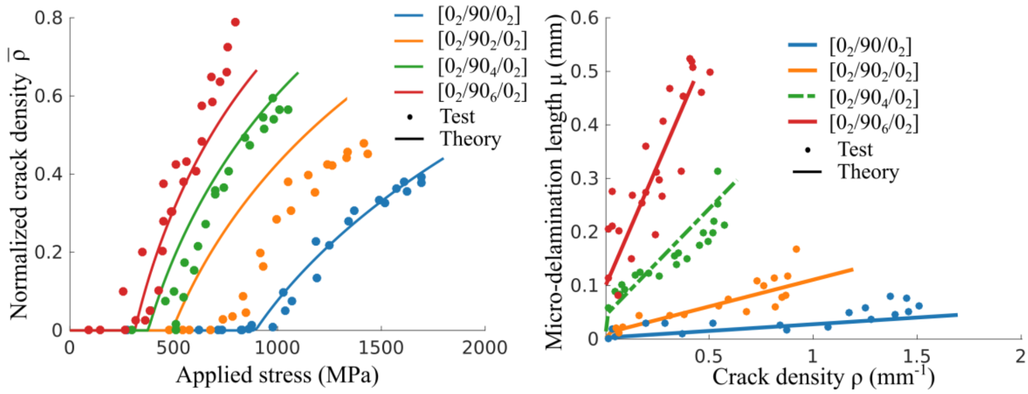

Figure 2. Damage evolution in $[0_2/90_n/0_2]$ laminates subjected to tensile loading. Model parameters were identified on $[0_2/90/0_2]$ and $[0_2/90_6/0_2]$ and applied to $[0_2/90_2/0_2]$ and $[0_2/90_4/0_2]$.

Identification of *in-situ* in-plane shear strength is performed on a $[+45/-45]_{2s}$ specimen subjected to tensile loading. As damage onset threshold Y_0 has been previously identified, these strengths are then used to determine coefficient a_{26} of Eq. 3 for each considered ply thickness.
Identifications on $[0/90n/0]$ and $[+45/-45]_{2s}$ are performed simultaneously to identify the α coefficient of damage evolution law (see Eq. 4). Fig. 3 shows the non-linear macroscopic stress-strain behavior and the damage evolution simulated with the model. Non-linear behavior prior to matrix cracking is described thanks to the micro-damage variable δ_2 introduced in the viscoelastic formulation.

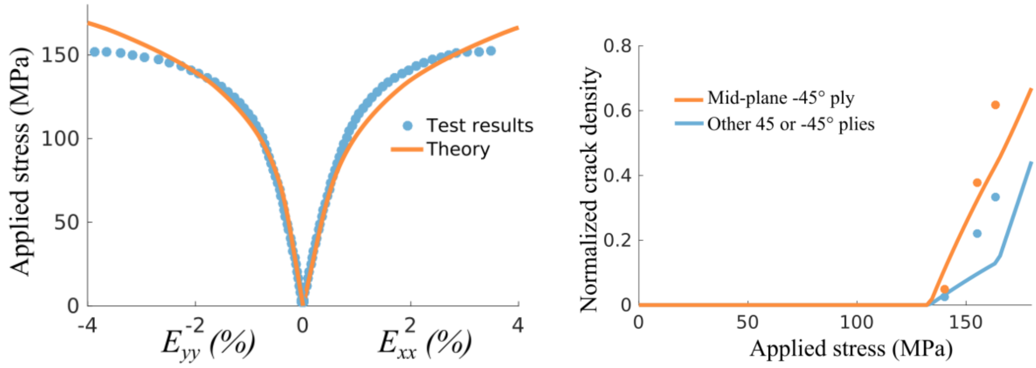

Figure 3. Laminate macro stress-strain behavior and damage evolution in $[+45/-45]_{2s}$ laminate subjected to a tensile loading

In addition, creep tests on [90] and $[+45/-45]_{2s}$. laminates are needed to identify the viscoelastic part of this model (see Eq. 6). Using multiple stress levels while performing creep tests is necessary, especially for $[+45/-45]_{2s}$ laminates to determine micro damage evolution law parameters (see Eq. 7 and Eq. 8) and its stress threshold where viscosity becomes non-linear, which is required to compute coefficient a_{26m}.

3.2. Predictive capabilities

Once this model has been identified, predictive capabilities to describe damage initiation and evolution are demonstrated on quasi-isotropic laminates. The first test case consists in a typical eight-ply laminate, representative of industrial configurations, in which the midplane is a 90° ply. Damage in this ply is compared with experimental data in Fig. 4. Damage onset and kinetics are well described by this approach.

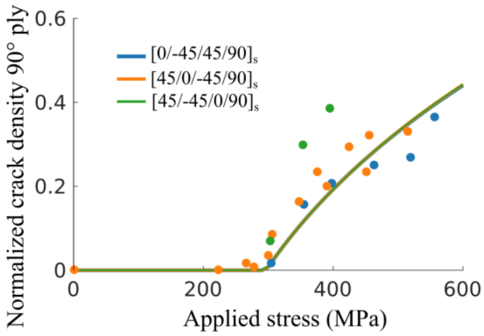

Figure 4. Damage in the 90° ply of 3 quasi-isotropic laminates under tensile load

The second test case consists in damage prediction of $[0_2/\text{-}60_2/60_2]_s$ and $[0/\text{-}60_2/0/60_2]_s$ laminates, where damage evolution are shown in Fig. 5. Damage onset and kinetics in the 60° ply are satisfactory compared to experimental data.

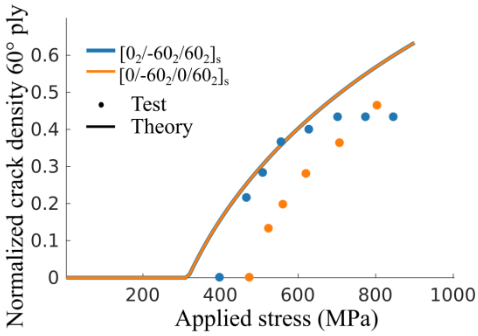

Figure 5. Damage model predictive capabilities on $[0/\text{-}60/60]_s$ and $[0/\text{-}60/0/60]_s$ laminates

Nevertheless, damage evolution was shown to be dependant of the stacking sequence in these configurations [3,10]. These effects of stacking sequence cannot be captured with a continuum damage model that remains local at the ply scale.

3.3. Finite elements modelling

The presented model is written at the ply scale, the chosen finite-element spatial discretization consists in modelling each ply by one volumic element in the thickness. In the following, fully integrated quadratic elements were chosen. A model comparison between the approach proposed by ONERA for the WWFE [1] and this new approach was performed on a quasi-isotropic $[45_4/90_4/\text{-}45_4/0_4]_s$ laminate. Viscous behaviors were omitted in these simulations as compared models have different formulations. Predicted normalized crack density for each ply is represented in Fig. 6 for both models.
Though damage locations remain similar, the damage pattern obtained with the previous approach is more localized. This can be explained by the softening behaviour of the WWFE approach (mesh dependency is however avoided through delay effect regularization). In both approaches, damage pattern in 90° ply is highly influenced by adjacent 45°/-45° plies. It is important to note that computational time for the current model was five times lower than for the WWFE approach, while the predictions remain rather similar.

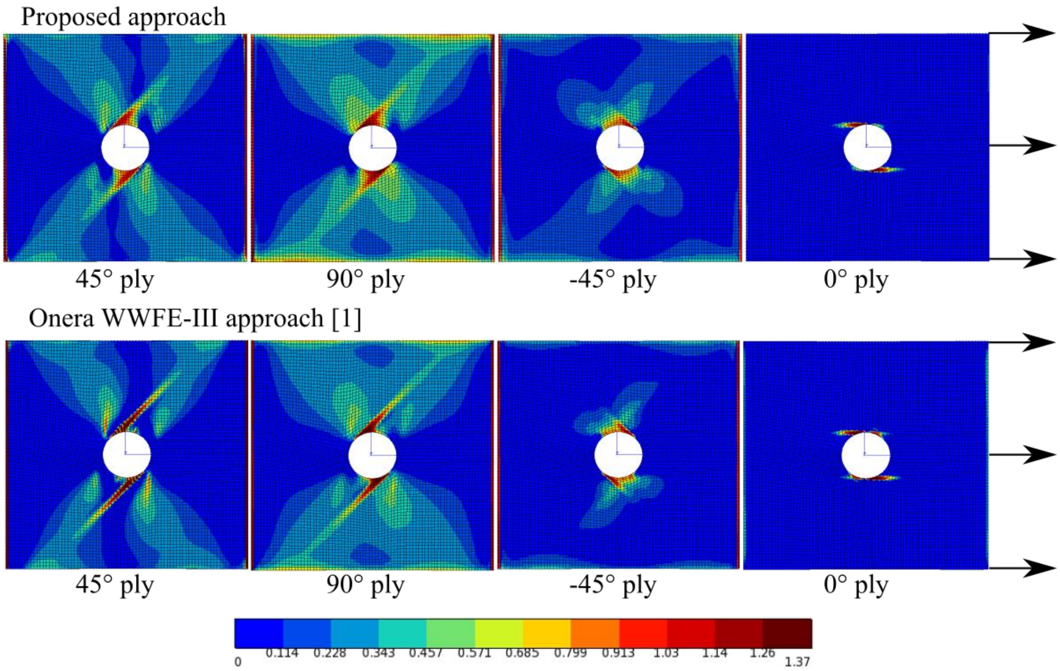

Figure 6. Comparison of predicted normalized crack density between the approach and ONERA WWFE-III approach [1]

The derivation of the tangent stiffness operator shows that the current model does not exhibit strain softening since second order tensor $\frac{\partial \bar{\rho}}{\partial \underline{\sigma}}$ is always positive definite. No mesh dependency is thus expected. However, Fig. 7 exhibits spurious oscillations in damage field. This problem may go undetected if quantities such as stress, strain or damage are visualized through interpolated nodal values or averaged at the centre of the elements.

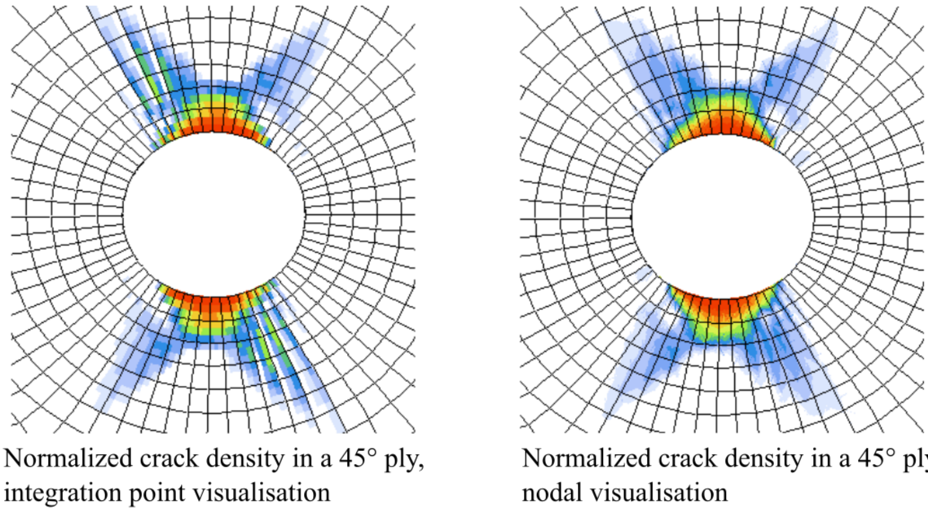

Figure 7. Integration point and nodal (extrapolated and interpolated) visualisation of damage in a 45°ply of $[+45/-45]_{2s}$ laminate

These numerical problems arise from a material instability which is characterized at some integration points by $\dot{\underline{\sigma}}:\dot{\underline{\varepsilon}} < 0$. Material instability can indeed occurs when the material tangent operator is not positive-definite [11]. For non-softening models, which can not induce loss of ellipticity (and the consequent mesh dependency issues), this can occur if the tangent operator is non-symmetric [12]. A reguralization method is to be considered.

4. Conclusions

In order to predict damage on a wide range of open-hole structure configurations, a new continuum damage model is presented. It relies on a complex physically-based model developed at ONERA for the WWFE, emphasis has been put here to propose a more robust approach, with a fair level of complexity.

This model is able to describe damage onset and kinetic in different laminates with different ply thicknesses. First computations on quasi-isotropic laminate show that matrix crack densities are accurately described. Despite this model does not exhibit strain softening, numerical difficulties related to the material loss of stability occur. A regularization method will be mandatory to overcome this difficulty.

In order to predict the strength of open-hole plate subjected to tensile loading on a wide range of industrial configurations, the present approach will be enhanced to accurately describe delamination and fibre failure.

Acknowledgement

The authors gratefully acknowledge the french DGAC for financially supporting this work.

References

[1] Laurin, F., Carrere, N., Huchette, C., & Maire, J. F. A multiscale hybrid approach for damage and final failure predictions of composite structures. *Journal of Composite Materials*, *47*(20-21), 2713-2747, 2013.

[2] Abisset, E., Daghia, F., & Ladevèze, P. On the validation of a damage mesomodel for laminated composites by means of open-hole tensile tests on quasi-isotropic laminates. *Composites Part A: Applied Science and Manufacturing*, *42*(10), 1515-1524, 2011.

[3] Huchette, C., Sur la complémentarité des approches expérimentales et numériques pour la modélisation des mécanismes d'endommagement des composites stratifiés. *Doctorate thesis of Université Paris 6*, 2005.

[4] Arteiro, A., Catalanotti, G., Melro, A. R., Linde, P., & Camanho, P. P, Micro-mechanical analysis of the in situ effect in polymer composite laminates. *Composite Structures*, *116*, 827-840, 2014

[5] Ladeveze, P., & Lubineau, G., An enhanced mesomodel for laminates based on micromechanics. *Composites Science and Technology*, *62*(4), 533-541, 2002.

[6] Parvizi, A., Garrett, K. W., & Bailey, J. E., Constrained cracking in glass fibre-reinforced epoxy cross-ply laminates. *Journal of Materials Science*, *13*(1), 195-201, 1978.

[7] Chang, F. K., & Chen, M. H., The in situ ply shear strength distributions in graphite/epoxy laminated composites. *Journal of Composite Materials*, *21*(8), 708-733, 1987.

[8] Camanho, P. P., Dávila, C. G., Pinho, S. T., Iannucci, L., & Robinson, P., Prediction of in situ strengths and matrix cracking in composites under transverse tension and in-plane shear. *Composites Part A: Applied Science and Manufacturing*, *37*(2), 165-176, 2006.

[9] Schieffer, A. Modélisation multiéchelle du comportement mécanique des composites à matrice organique et effets du vieillissement thermique. *Doctorate thesis of Université de Technologie de Troyes*, 2003.

[10] Laeuffer, H., Caractérisation et modélisation des réseaux de fissures pour la prédiction de la perméabilitédes réservoirs composites stratifiés sans liner. *Doctorate thesis of Arts et Métiers ParisTech, Bordeaux,* 2017.

[11] De Borst, R., Sluys, L. J., Muhlhaus, H. B., & Pamin, J., Fundamental issues in finite element analyses of localization of deformation. *Engineering computations*, *10*(2), 99-121, 1993.

[12] Forest, S., & Lorentz, E., Localization phenomena and regularization methods. *Local approach to fracture*, 311-371, 2004.